AMAS Course on Nondestructive Testing of Materials
NTM'02 – (pp.61–80) – Warsaw, May 20-22, 2002.

Nondestructive evaluation of stress states in components using ultrasonic and electromagnetic techniques

E. SCHNEIDER

Fraunhofer Institut
Zerstörungsfreie Prüfverfahren IZFP
Germany
schneider@fhg.izfp.de

Complementary to the established techniques to evaluate stress states, electromagnetic and ultrasonic techniques permit the evaluation of stresses in surface layers and in the bulk of components, respectively. One advantage of these techniques is the possibility of a fast evaluation of stress states, enabling a continuous analysis along traces to get an information about the stress distribution and the stress inhomogeneities. Both the electromagnetic and the ultrasonic techniques have been developed for different cases of application on homogeneous components and set-ups for the automated evaluation of stress states are in industrial use.

A disadvantage of both techniques is the influence of changes of microstructural states on the measuring quantities. In case of the electromagnetic techniques, calibrations have to be done, using representative samples in tensile test experiments. The quantitative evaluation of stress states using ultrasonic techniques preassumes the knowledge of the acousto-elastic constants. These constants describe the interdependency between the ultrasonic measuring quantities (sound velocity or time-of-flight) and the strain or stress states. It can be assumed that the microstructural states of e.g. the weld seam, of the heat affected zone and of the base material cause differences in the acousto-elastic constants.The influence of the microstructural state on the electromagnetic and acousto-elastic quantities has been studied using material samples cut from welded plates. Depending on the steel grade, on the sheet thickness and on the welding parameters, the microstructural state as well as the texture in and around the weld seam differs. It is found that the texture and microstructural influence on the acousto-elastic constants is not as significant as it was expected. Applying multi-parametric regression algorithms on the electromagnetic quantities, the microstructural states influence can be suppressed. Using the evaluated acousto-elastic constants the stress states in and around welding seams were mapped. Comparisons with the results of an established technique show the reliable application of both techniques.

1. Ultrasonic technique

1.1. Physical background

The state of art is described e.g. in the handbooks [1] and [2]. The major relationships are repeated. The equations show the influence of a three dimensional stress state on the relative changes of longitudinal and shear wave velocities:

$$\frac{v_{ii} - v_L}{v_L} = \frac{A}{C}\sigma_i + \frac{B}{C}(\sigma_j + \sigma_k), \tag{1.1a}$$

$$\frac{v_{ij} - v_T}{v_T} = \frac{D}{K}\sigma_i + \frac{H}{K}\sigma_j + \frac{F}{K}\sigma_k, \tag{1.1b}$$

$$\frac{v_{ik} - v_T}{v_T} = \frac{D}{K}\sigma_i + \frac{F}{K}\sigma_j + \frac{H}{K}\sigma_k \tag{1.1c}$$

The first index of the velocity v gives the direction of propagation, the second the direction of polarization of the ultrasonic wave. i, j, k are the axes of a Cartesian coordinate system. v_L and v_T are the longitudinal and shear wave velocities in the isotropic, stress free state. λ and μ are the Lamé constants (second order elastic constants), l, m and n are the third order elastic constants of the material.

A, B, C, D, H, F and K are combinations of the II and III order elastic constants of the material [2, 3]:

$$\begin{aligned}
A &= 2(\lambda+\mu)(4m+5\lambda+10\mu+21) - 2\lambda(21+\lambda),\\
B &= 2(21+\lambda)(\lambda+\mu) - \lambda(21+\lambda) - \lambda(4m+5\lambda+10\mu+21),\\
C &= 4\mu(\lambda+2\mu)(3\lambda+2\mu),\\
D &= 2(\lambda+\mu)(\lambda+m+4\mu) - \lambda(2\lambda+2m+2\mu-n/2),\\
H &= 2(\lambda+\mu)(\lambda+m+2\mu) - \lambda(2\lambda+2m+4\mu-n/2),\\
F &= 2(\lambda+\mu)(\lambda+m-n/2) - \lambda(2\lambda+2m+6\mu),\\
K &= 4\mu\sigma^2(3\lambda+2\mu).
\end{aligned} \tag{1.2}$$

A/C and B/C etc., determine the influence of one of the principal stresses. Later on, the inverse values C/A and C/B etc., are used in order to give the value of the individual principal stress which causes a 0.1% change of the above mentioned relative difference of velocities.

Using Eqs. (1.1b) and (1.1c), the following equations of the ultrasonic birefringence effect can be formulated:

$$\begin{aligned}
\frac{t_{ik}-t_{ij}}{t_{ij}} &= \frac{4\mu+n}{8\mu^2}(\sigma_j-\sigma_k) = S(\sigma_j-\sigma_k),\\
\frac{t_{ji}-t_{jk}}{t_{jk}} &= \frac{4\mu+n}{8\mu^2}(\sigma_k-\sigma_j) = S(\sigma_k-\sigma_i),\\
\frac{t_{kj}-t_{ki}}{t_{ki}} &= \frac{4\mu+n}{8\mu^2}(\sigma_i-\sigma_j) = S(\sigma_i-\sigma_j),
\end{aligned} \tag{1.3}$$

with $S = \frac{4\mu+n}{8\mu^2}$.

The advantage of applying the birefringence effect (Eqs. 1.3) is the independence from the measurement of the ultrasonic path length and the fact, that there is only one III order elastic constant needed and this constant is very weakly influenced by microstructural properties. In order to evaluate stress states of surface near layers (about 1 to 9 mm of thickness) the application of a skimming longitudinal (SL) and/or a SH_0 wave is recommended. Adjusting the direction indexes according to the directions of the principal axes and the propagation and vibration directions, Eqs. (1.1) can be applied.

The generalizations of the Eqs. (1.1) to propagation directions not along the principal axes describe the angular dependence of the relative velocity changes of the skimming longitudinal (v_{SL}) and of the SH_0 (v_{SH}) wave:

$$\begin{aligned}
\frac{v_{SH}(\Theta)-v_T}{v_T} &= \left(\frac{D+F}{2K}\right)(\sigma_i+\sigma_j) + \left(\frac{D-F}{2K}\right)(\sigma_i+\sigma_j)\cos 2\Theta,\\
\frac{v_{SL}(\Theta)-v_L}{v_L} &= \left(\frac{A+B}{2C}\right)(\sigma_i+\sigma_j) + \left(\frac{A-B}{2C}\right)(\sigma_i+\sigma_j)\cos 2\Theta,
\end{aligned} \tag{1.4}$$

where σ_i and σ_j are the principal in plane stresses and Θ is the angle between propagation direction and σ_i. The application of a Rayleigh wave can not be recommended as explained in [2, 3].

1.2. Influence of microstructural state

The microstructure determines the elastic behavior of a material and hence the elastic and acousto-elastic constants. They have been evaluated for different steel grades. The influence of microstructural changes on the values of the combination of II and II order elastic constants is not as strong as it has been expected.

Table 1 summarizes the coefficients shown in the Eqs. (1.1). The unit of the coefficients C/A, C/B etc. is [MPa/0.1%].

TABLE 1.

Material	C/A	C/B	K/D	K/H	K/F	$1/S$
Railroad rail	-66 ± 10%	/	-565	-127 ± 7%	/	-123 ± 5%
Type UIC 60 different manufacturers, straightened	-67	/	-672	-132	/	-133
and not straightened	-67	/	-672	-132	/	-137
	-70	/	-799	-136	/	-141
	-71	/	-830	-137	/	-142
Steel S255N	-150 ± 25%	504	2011	-176	1743	-160
Steel C 105 W1	-190	350	/	-180	787	-147
17CrNiMo 6	-137 ± 20%	485	/	-162	740	-133
20CrNiMo 13	-81 ± 11%	769	-730	-133 ± 6%	/	-118 ± 5%
24CrMo5V	-81	/	-1031	-143	/	-149
24CrMo5V	-80	/	-1554	-148	/	-157
30CrMoNiV 5 11	-91	/	/	-158	/	-163
22NiMoCr 3 7	-133 ± 13%	/	1816	-180 ± 7%	/	-166 ± 6%
22NiMoCr 3 7	-122	1013	/	-173	/	-164
22NiMoCr 3 7	-109	723	/	-162	/	-163
24NiCrMoV 14 5	-204 ± 17%	929	588	-220 ± 8%		-227 ± 7%
Ni-Steel	-89 ± 11%	/	/	-152	/	-155
15MnNi 6 3	-91	903	/	-145	/	-136
X6CrNi 1811	-68 ± 11%	/	/	-177 ± 8%	-141	-108 ± 8%
X6CrNi 1811	-78	/	734	-189	-149	103
WC-Co Sintered Met.	-312 ± 12%	/	/	-502 ± 8%	/	-484 ± 6%
WC-Co Sintered Met.	-278	/	/	-475	/	-470

TABLE 2.

Microstructure	C/A	C/B	K/D	K/H	K/F	$1/S$
Ferrite-Pearlite Ferrite 50%	-75	1920	-826	-136	/	-136
Ferrite 30-40% + Intermediate	-70	1755	-735	-133	1724	-144
Intermediate	-80	1389	-1064	-141	/	-142
Intermediate + Widmanstätten	-101	1639	/	-165	2273	-178
Intermediate + Retained Austenite	-84	1563	-1449	-146	/	-150
Error	≤ ± 10%	/	/	≤ ± 10%	/	≤ ± 2%

Since the welding process causes a strong change of microstructure and since welding stress is of particular interest, the material dependent constants have been evaluated using samples cut from a welded 15MnNi 6 3 steel plate. Table 2 gives the coefficients.

The microstructure was characterized by metallography. The second order elastic constants have been found to be the same for all the samples: $\lambda = 110\,\text{GPa}$, $\mu = 81\,\text{GPa}$. The inaccuracy is about $\pm 1\%$. The second order elastic constants have been found to remain unchanged after hardening treatments also. The hardness of different steel samples was modified. The coefficients are given in Table 3.

TABLE 3.

Material Hardness	C/A	C/B	K/D	K/H	K/F	$1/S$
20CrNiMo 13						
160 HB	-81	769	-730	-133	/	-118
437 HB	-73	763	-578	-127	/	-112
17CrNiMo 6						
304 HB	-79	705	-691	-131	1748	-122
342 HB	-73	606	-569	-126	/	-125
415 HB	-133	/	/	-183	847	-150
22NiMoCr 3 7						
269 HV10	-87	537	-1154	-143	2096	-153
286 HV10	-94	519	-1717	-147	2077	-159
368 HV10	-87	431	-941	-137	/	-142
400 HV10	-94	458	-1219	-141	/	-138
Error	$\leq \pm 10\%$	/	/	$\leq \pm 7\%$	/	$\leq \pm 4\%$

After plastic deformation to about 11%, the second order elastic constants were found to be unchanged within the measuring inaccuracy of about $\pm 1.5\%$; $\lambda = 111\,\text{GPa}$, $\mu = 82\,\text{GPa}$. The coefficients have changed, see Tables 4 and 5.

TABLE 4.

22NiMoCr 3 7 Plastic deformation Dislocation density	C/A	C/B	K/D	K/H	K/F	$1/S$
ε_{pl}: 1%; $1.4 \cdot 10^{10}\,\text{cm}^{-2}$	-98	/	/	-165	/	-177
ε_{pl}: 5%; $2.4 \cdot 10^{10}\,\text{cm}^{-2}$	-47	1319	-281	-103	-469	-133
ε_{pl}: 10%; $3.1 \cdot 10^{10}\,\text{cm}^{-2}$	-46	461	-252	-100	-342	-141
Error	$\leq \pm 12\%$			$\leq \pm 7\%$	/	$\leq \pm 5\%$

TABLE 5.

Material Elastic Anisotropy [%]		C/A	C/B	K/D	K/H	K/F	$1/S$
EStE 690 VA	R	-74	935	-505	-126	741	-107
0.15%	W	-82	765	-704	-135	/	-122
StE 240.7 TM	R	-76	759	-589	-129	/	-117
1.2%	W	-108	922	-5044	-159	/	-144
StE 240.7 TM	R	-72	561	-433	-120	789	-104
1.8%	W	-121	/	4421	-172	1520	-154
StE 385.7 TM	R	-60	475	-296	-107	930	-96
4.5%	W	-95	793	-2110	-155	/	-167
StE 445.7 TM	R	-55	358	-230	-97	716	-86
5.5%	W	-97	613	-1178	-147	/	-133
StE 550.7 VA	R	-43	385	-175	-85	1325	-80
6.2%	W	-105	/	2419	-176	/	-200
Error		$\leq \pm 5\%$			$\leq \pm 10\%$		$\leq \pm 3\%$

Since pipes are mainly produced from rolled plates, the influence of rolling texture on the coefficients is of interest. Samples were cut parallel (R) and perpendicular (W) to the rolling direction of steel grades, often used for pipeline tubes.

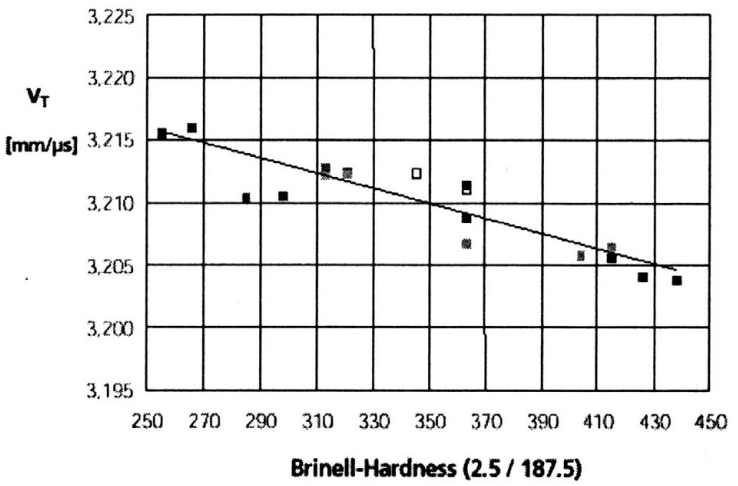

FIGURE 1. Shear wave velocity v_T versus Brinell hardness of different samples of steel grade 17CrNiMo 6.

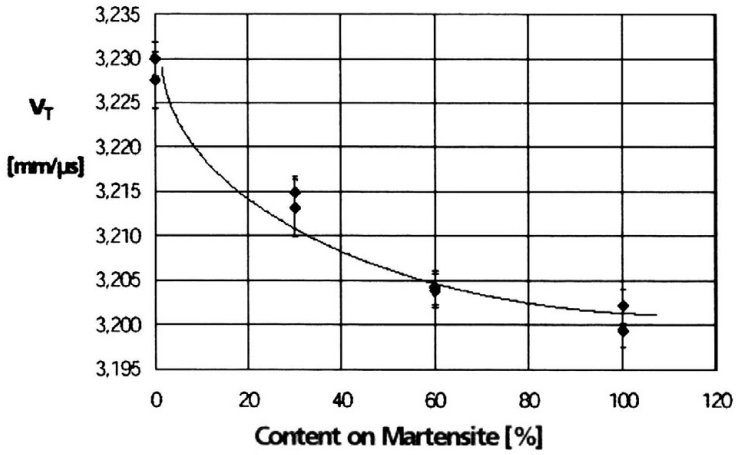

FIGURE 2. Shear wave velocity v_T versus content on martensite of 22NiMoCr 3 7 steel samples.

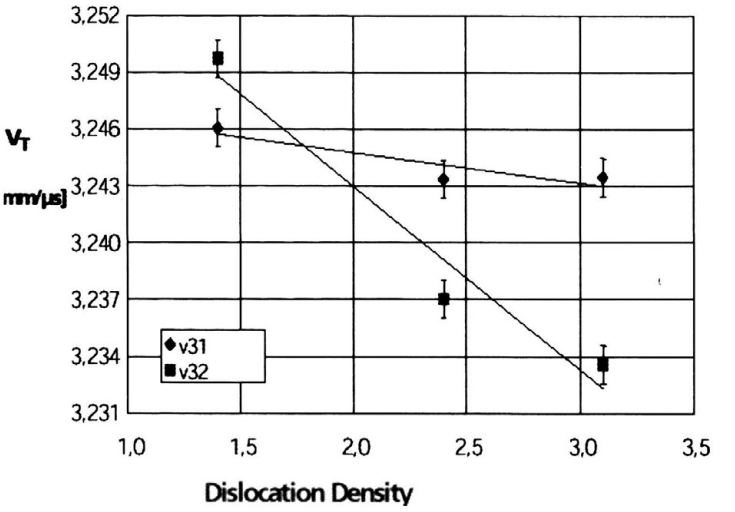

FIGURE 3. Shear wave velocity v_T versus dislocation density $[\cdot 10^{10}\,\mathrm{cm}^{-2}]$ of 22NiMoCr 3 7 steel samples.

As seen in Eqs. (1.1), the sound velocity representing the stress free state is needed for the quantitative stress analysis. The velocity representing the stress free state is found to be influenced by microstructural changes.

The changes of the longitudinal wave velocity is in the same order of magnitude [2, 3]. The strategy is to find a position at the component of interest

with a representative microstructural state and a small residual stress value. The other possibility is to take measurements across a part of the component, large enough in order to take advantage of the stress equilibrium conditions. The influence of texture on the measuring quantities causes difficulties. Different approaches are developed in order to discriminate the texture influence or to take it into account [1, 2, 3]. In general it can be stated that more homogeneous the texture is, more space to perform measurements using different types of ultrasonic waves is available. Thus the texture influence can be discriminated or taken into account. The most appropriate strategy has to be found for each individual case of application.

1.3. Set-ups

Set-ups for the automated data acquisition and evaluation of stress states are available. Since the acousto-elastic effect is small, and since there are different types of ultrasonic waves which principally can be applied and since there are different influencing parameters to be taken into consideration, there is no general solution for all cases of application. But in each case, the ultrasonic time-of-flight has to be measured with high accuracy, the position of the sensor has to be taken and in some cases the temperature of the component has to be also measured. There are appropriate systems on the market. For specific applications, ultrasonic techniques were developed and set-ups were optimized for the daily use in workshops [1, 2, 3].

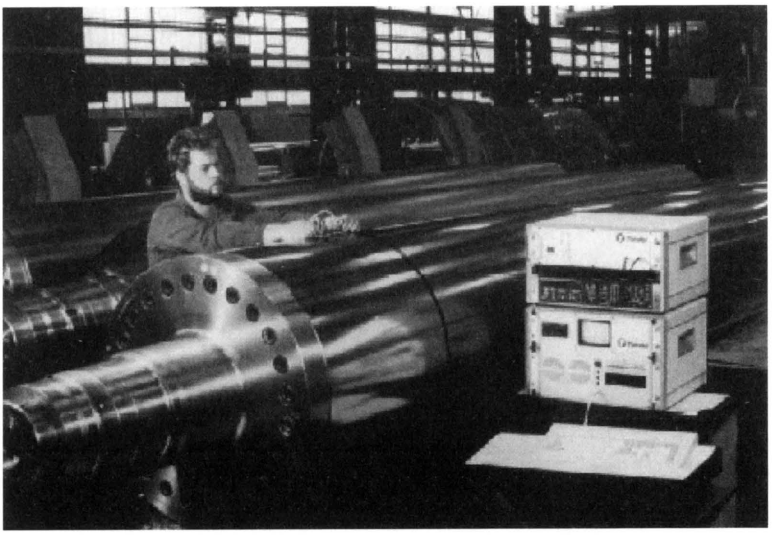

FIGURE 4. The system AUSTRA for the analysis of surface stress states

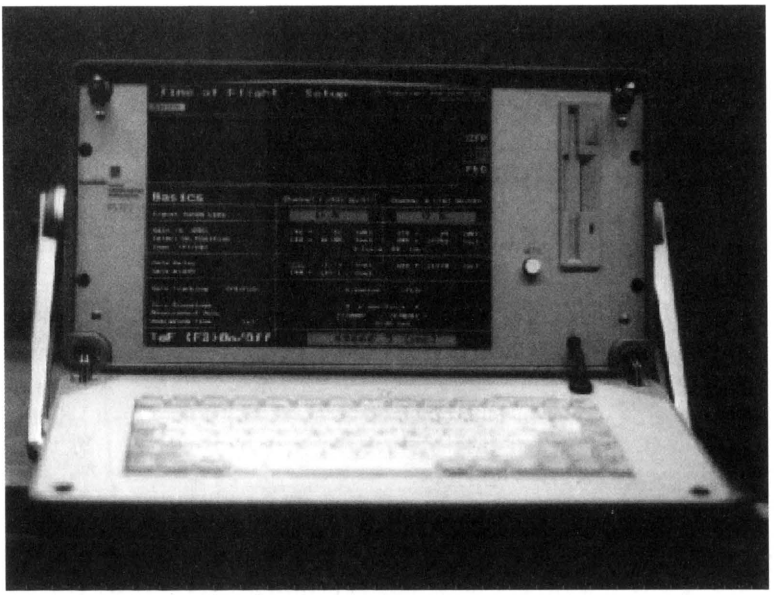

FIGURE 5. The new portable system AUSTRA.

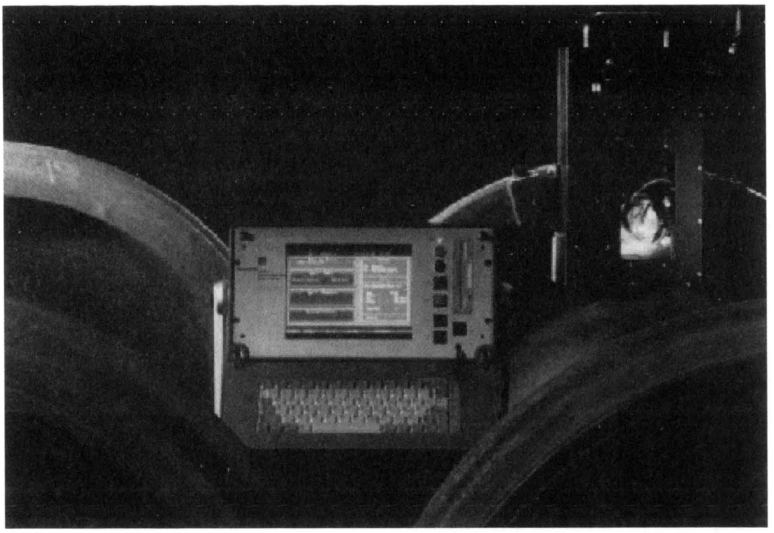

FIGURE 6. The UER-T system for stress analysis on railroad wheels.

1.4. Sensors

Ultrasonic longitudinal and shear wave transducers of different center frequencies and sizes are on the market. Electromagnetic ultrasonic transducers (EMATs) are becoming smaller in size and more efficient and facilitate the automated data acquisition using manipulator systems. However, there is a need to optimize the transducers for each individual application. It is most often the geometry of the component and the limited space around the area of interest which makes a specific optimization of the sensors necessary.

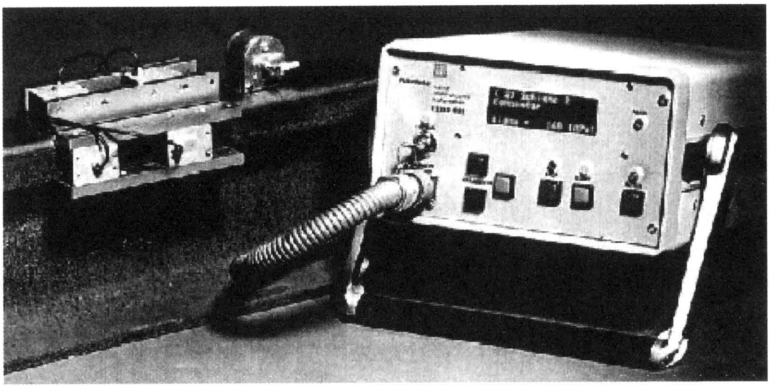

FIGURE 7. The UES system, a 3 channel system for stress analysis on long products.

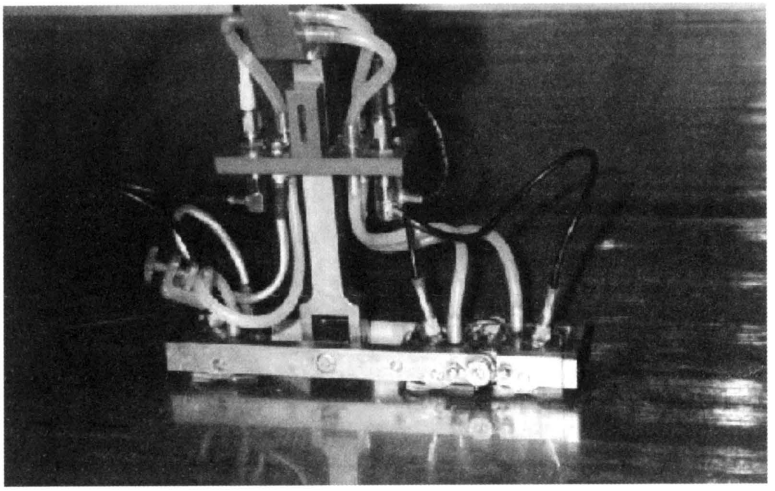

FIGURE 8. Combination of three piezoelectric longitudinal wave transducers, one transmitter and two receivers, for the surface stress analysis using a skimming longitudinal wave.

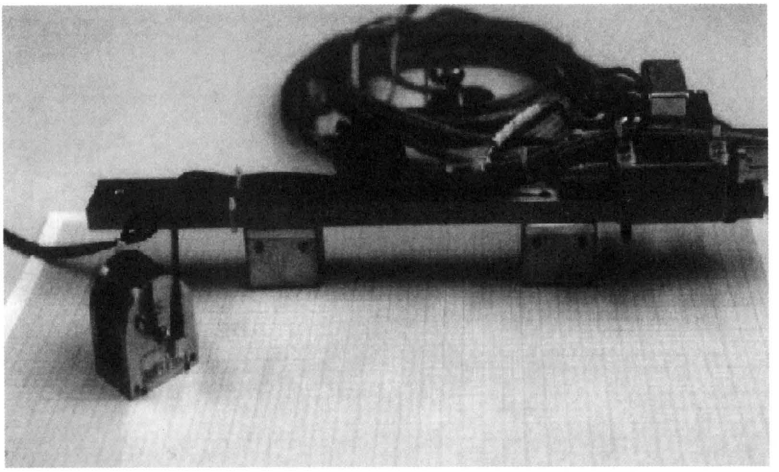

FIGURE 9. EMAT transducer for normal incident linearely polarized shear wave (front left) used for bulk stress analysis and a EMAT transmitter-receiver system for surface stress analysis using a SH_0 wave.

2. Results of ultrasonic stress analysis

Figure 10 shows the hoop stress along the length of a wheel shaft. The shaft has a central bore hole along its length. The ultrasonic sensor is moved in the hole along the length. The situation can be compared with a measurement inside a pipe. A SH_0 wave is used which vibrates along the hoop direction. The figure shows the results before and after different treatments to reduce the hoop stress. Figures 12 and 13 display the welding stress parallel and perpendicular to the welding seam in a 4 mm thick Al sheet. Along two measuring traces, the ultrasonic results are compared with those of hole drilling technique.

3. Electromagnetic techniques

3.1. Fundamentals

There is no evaluation equation connecting the stress or strain state with the electromagnetic and magneto-elastic quantities, as it is the case between the stress or strain state and the velocities of ultra-sonic waves. Since all electromagnetic and magneto-elastic quantities of a ferromagnetic material are influenced by stress and microstructure and their changes, the measuring quantities need to be calibrated using samples with a representative microstructural state. A calibration process using measuring quantities based

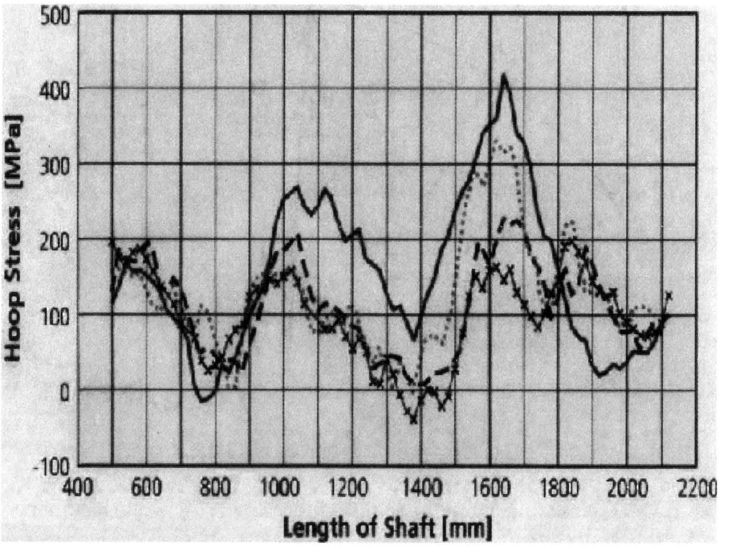

FIGURE 10. Hoop stress along the length of a hollow wheel shaft after different treatments to reduce the stress.

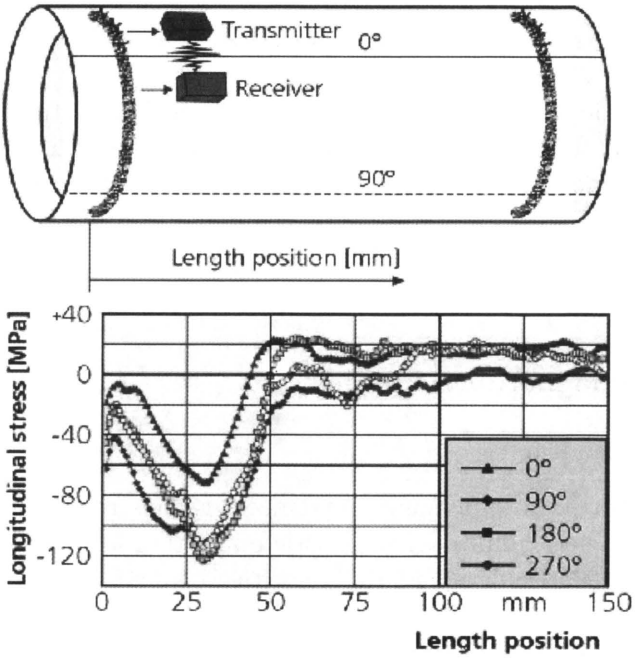

FIGURE 11. Longitudinal stress distribution in a welded pipe.

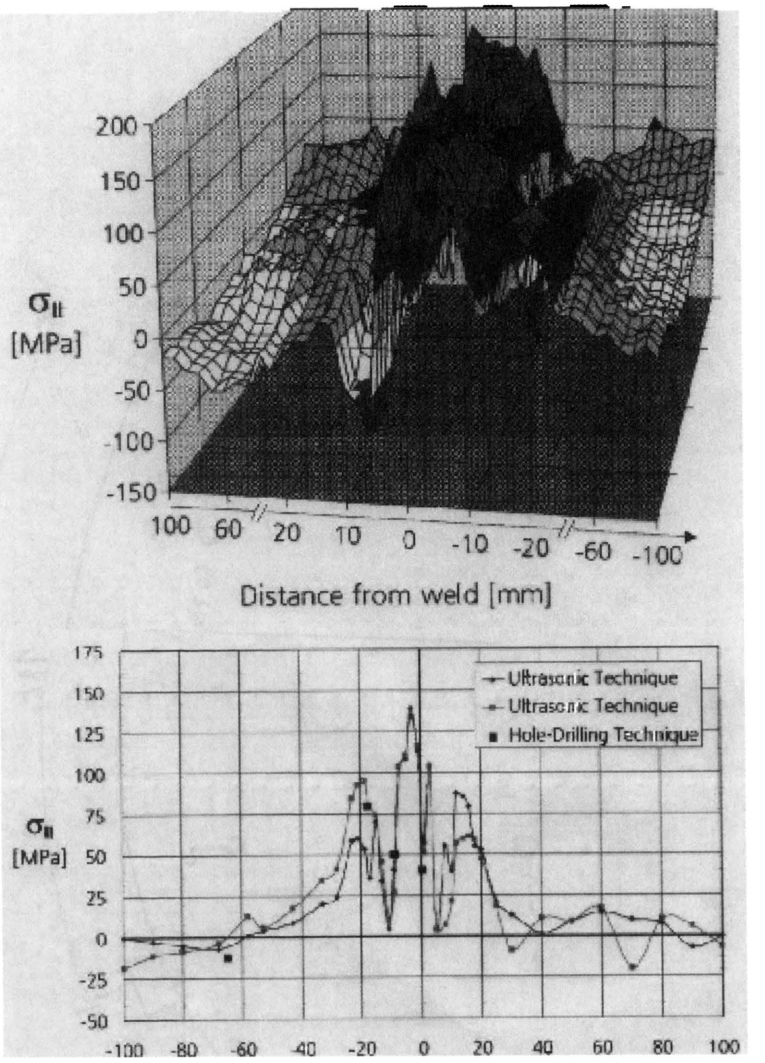

FIGURE 12. Welding stress parallel to seam in an Al-plate.

on different electromagnetic and magneto-elastic interactions with the stress and the microstructural state of the component results not only in a higher accuracy of the result but also in a minimized influence of disturbing parameters. In order to minimize the influence of disturbing parameters like inhomogeneities of the microstructure or the distance between the sensor and the components surface (lift-off), the calibration measurements have to include the variations of these parameters. The stress dependencies of the

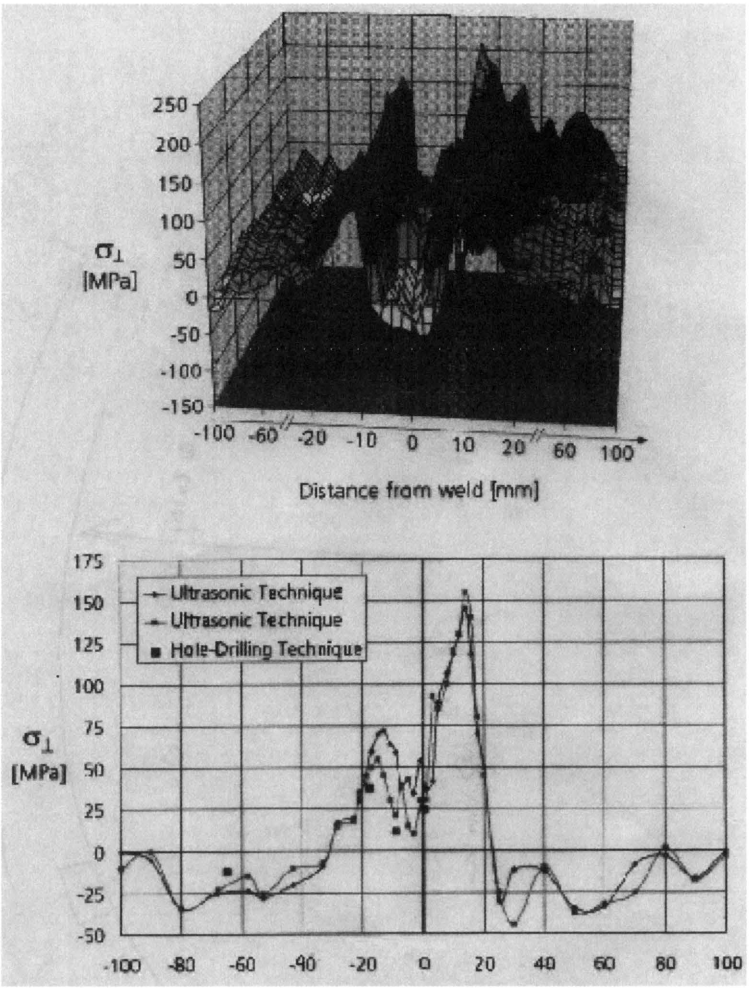

FIGURE 13. Welding stress perpendicular to seam.

electromagnetic and magneto-elastic quantities are measured using samples with different micro-structural states (like weld seam, heat affected zone, base material) in a tensile test or bending experiment. The variation of the lift-off is a further parameter during the calibration process. The calibration function is calculated by a multiple regression analysis. The advantage of this procedure is that the microstructural influences and the lift-off are taken into account. Hence the stress state can be evaluated even if the microstructure or the lift-off change along the measuring traces.

The electromagnetic and magneto-elastic quantities, frequently used for stress analysis are measuring parameters derived from Barkhausen noise (BN),

incremental permeability (μ_Δ) and from the upper harmonics analysis of the time signal of the tangential magnetic field strength $H_t(t)$ [4, 5]. Measuring parameters are:

$M_{\max}$ – maximum of BN,
H_{CM} – coercivity of BN,
ΔH_M – width of $M(H)$ envelope at distinct M-values,
$\mu_{\Delta\,\max}$ – amplitude of μ_Δ,
$H_{\mathrm{C}\mu}$ – coercivity of μ_Δ,
ΔH_μ – width of $\mu_\Delta(H)$ at a distinct μ_Δ-value,
K – distortion factor,
H_{CO} – coercivity.

3.2. Set-up and sensor

The set-up and the sensor allow the simultaneous measurement of the above mentioned measuring parameters. Set-up and sensor are introduced into the market as 3MA Unit and 3MA Sensor. 3MA is the abbreviation for **M**icromagnetic **M**ultiparameter **M**icrostructure and Stress **A**nalyzer Technique.

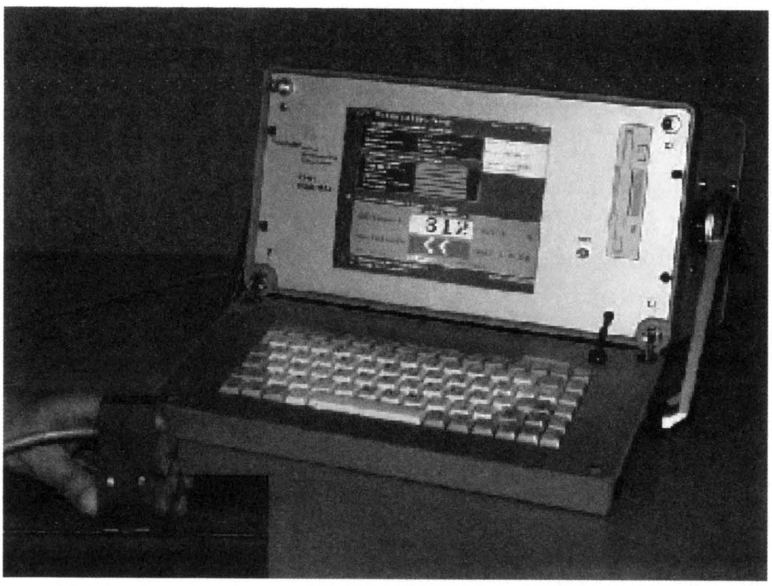

FIGURE 14. 3MA set-up.

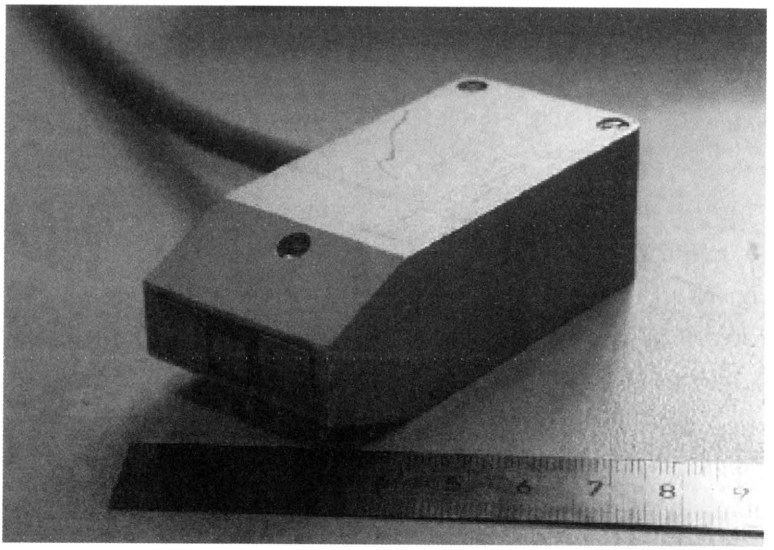

FIGURE 15. 3MA sensor.

3.3. Results

In order to prepare measurements of the longitudinal stress in a moved steel strip, the calibration was done in a tensile test experiment. During the intended on-line measurements in the mill, the distance between the surface of the strip and the sensors will change between about 1 and 3 mm. Hence, the mentioned calibration has to be done at the lift-off values between the specified limits. The calibration function uses 12 electromagnetic and magneto-elastic quantities, derived from the incremental permeability (μ_Δ) and from the upper harmonics analysis of the time signal of the tangential magnetic field strength $H_t(t)$.

In order to prove the reliability of the calibration function, a sample of the strip is stressed. The stress is controlled by strain gauge measurements and the 3MA technique is applied at different lift-offs. Figure 16 displays the number of the readings of the evaluated 3MA stress values. The applied stress was 40 MPa, the lift-off was changed between about 1 and 3 mm. The mean value of the 3MA results is 41 MPa, 90.2% of the evaluated results show values in the range of 41 MPa $\pm$ 3 MPa, 96.8% are in the range of 41 MPa $\pm$ 4 MPa, and 99.4% are in the range of 41 MPa $\pm$ 5 MPa.

Figure 17 shows a result taken at the moved strip in the mill. The thickness of the strip is 2.5 mm. The strip speed was about 120 m per minute. A 3MA result was taken every second. The stress profile was measured during

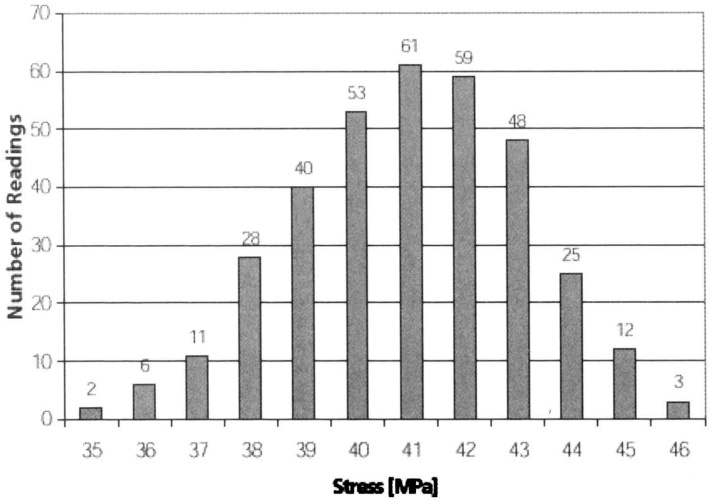

FIGURE 16. Distribution of the 3MA results on a steel strip under an applied load of 40 MPa.

FIGURE 17. Results of a 3MA stress analysis on a moved strip.

16 minutes and the longitudinal strip tension was changed for test reasons by the mill operator.

Microstructural changes might be characterized by the hardness values. Using samples with different hardness (meaning microstructure) in a tensile test or bending experiment, the influence of the stress was calibrated. The

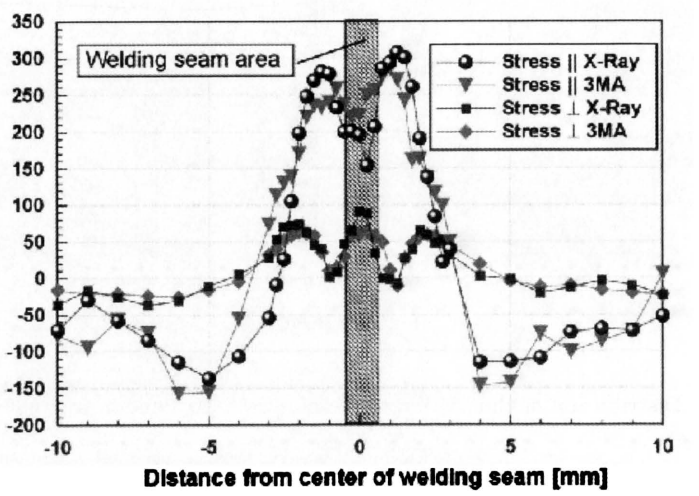

FIGURE 18. Principal stresses in a welded sheet # 1.5 mm, evaluated by 3MA and X-ray technique.

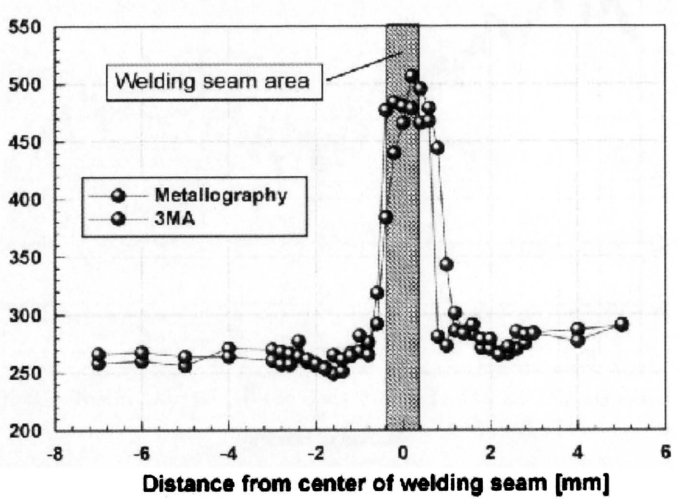

FIGURE 19. Vickers hardness in the welded sheet of 1.5 mm of Vhickness, evaluated by 3MA-technique and metallography.

above mentioned measuring quantities are taken and a nonlinear regression algorithm was applied in order to evaluate the calibration function. Figure 18 displays the principal stresses across a weld in a sheet of 1.5 mm of thickness. For comparison reasons, the values evaluated by X-ray diffraction technique are also shown.

After the corresponding calibration is made, the hardness can also be evaluated (Fig. 19) and compared with the hardness determined by metallography [6].

4. Summary

There is a profound understanding of the physical background of the ultrasonic and electromagnetic techniques to evaluate stress states in components. The relevant material dependent acousto-elastic constants are known for a large number of steel and Al-alloys, experimental results on the influence of texture and microstructural states on the elastic constants are available for different cases of application. The strategy towards the appropriate calibration of different electromagnetic and magneto-elastic quantities for stress analysis is known and proven. Rules are known for the appropriate technique to minimize disturbing influences like changes of microstructural state and lift-off.

However, neither the ultrasonic nor the electromagnetic set-ups can just be taken from the shelf and applied. The technique and the lay-out of the sensor has to be adapted to the individual case of application. Since both techniques allow a locus continuous data acquisition with acquisition rates in the range of 50 till 100 readings per second, both techniques are suited to analyze large areas of a component. The next step towards a user friendly unit is the design of sensors allowing the data acquisition of both, ultrasonic and electromagnetic, magneto-elastic quantities and the development of a software package which combines the results of both techniques with other side information like e.g. the stress equilibrium condition.

References

1. R.B. THOMPSON, W.Y. LU, A.V. CLARK JR., *Ultrasonic Methods. Handbook of Measurements of Residual Stresses*, pp.149-178, J. Lu (Ed.), Society for Experimental Mechanics Inc., The Fairmont Press Inc., Lilburn, USA 1996.

2. E. SCHNEIDER, Ultrasonic techniques, in: V. Hauk (Ed.), *Structural and Residual Stress Analysis by Nondestructive Methods*, pp.522-563, Elsevier Science B.V., Amsterdam 1997.

3. E. SCHNEIDER, *Untersuchung der materialspezifischen Einflüsse und verfahrenstechnische Entwicklungen der Ultraschallverfahren zur Spannungsanalyse an Bauteilen*, Fraunhofer IRB Verlag, Stuttgart 2000.

4. W.A. THEINER, Micromagnetic techniques, in: V. Hauk (Ed.): *Structural and Residual Stress Analysis by Nondestructive Methods*, pp.564-589, Elsevier Science B.V., Amsterdam 1997.

5. R. KERN, R. MEYER, W.A. THEINER, B. VALESKE, Process integrated nondestructive testing of laser-hardened components, *Materials Science Forum*, Vol.210-213, pp.687-694, 1996.

6. W.A. THEINER, R. KERN, I. LEJEUNE, Grundlegende Untersuchungen zur orts- und zeitaufgelösten zerstörungsfreien Bestimmung mikrostructureller Eigenschaften, *DVS-Berichte Band*, Vol.205, pp.81-86, 1999.